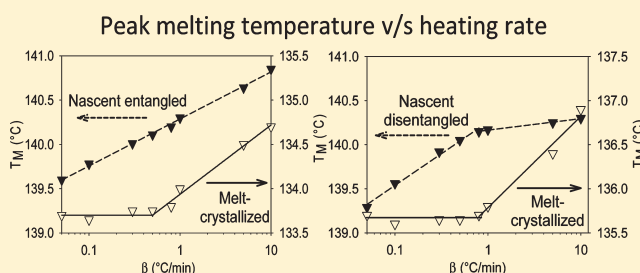


Influence of Amorphous Component on Melting of Semicrystalline Polymers

Anurag Pandey,^{†,‡} Akihiko Toda,^{||} and Sanjay Rastogi^{*,†,‡,§}[†]Department of Materials, Loughborough University, Loughborough, LE11 3TU, U.K.[‡]The Dutch Polymer Institute (DPI), P.O. Box 902, 5600 AX Eindhoven, The Netherlands[§]Department of Chemical Engineering, Eindhoven University of Technology, P.O. Box 513, 5600 MB Eindhoven, The Netherlands^{||}Graduate School of Integrated Arts and Sciences, Hiroshima University, Higashi-Hiroshima 739-8521, Japan

Supporting Information

ABSTRACT: Unlike inorganic and organic molecules, in semicrystalline polymers melting gets complicated because of the requirement of conformational transformation of the chain segments, where part of the same chain resides in the crystal and also in the amorphous phase. The chain segment residing in the amorphous part can be constrained, either due to adjacent or nonadjacent re-entry leading to a different nature of chain folding, and arising differences are observed in local chain mobility due to differences in topological constraints. Thus, different conformational possibilities in the amorphous region of the semicrystalline polymer has implications on melting temperature and the processes involved in the order to the disorder phase transformation. With a series of experiments on ultra high molecular weight polyethylene, where the topological constraints are tailored by adopting a different synthesis route, it is shown that melting behavior cannot be fully explained by Gibbs–Thomson equation only. Nonlinearity in melting temperature on heating rate invokes kinetics in the melting process, where depending on the heating rate melting can occur either via successive detachment of chains and their diffusion in the melt or by cluster melting. The role of superheating on melting process is also addressed.



INTRODUCTION

Melting in semicrystalline polymers is a complex process, where melting transition is not sharp and covers a broad temperature range and is correlated to the distribution of the crystal lamellae thickness. Thermodynamically, melting in solids is defined as a first-order transition (sharp) at the intersection of the Gibbs free energy of the solid and liquid state, which is only true if we consider equilibrium and infinite size of the phases involved. However, these conditions are not met in semicrystalline polymers such as polyethylene, either crystallized from solution or melt. These polymers possess lamellae crystal thickness of finite dimensions (10–30 nm) with lateral dimensions of at least an order of magnitude larger.^{1–6} Gibbs–Thompson equation in its simple form has been widely used to quantitatively describe the maximum melting temperature correlating the lamellae thickness

$$T_m = T_m^\infty \left[1 - \frac{2\sigma}{l\rho\Delta H_m} \right] \quad (1)$$

where T_m is the experimentally determined melting temperature, T_m^∞ is the equilibrium melting temperature for infinite size crystal (141.5 °C for polyethylene^{7,8}), σ is the end surface free energy for the folded planes, l is the crystal

lamellae thickness, ρ is the crystal density, and ΔH_m is the heat of fusion per unit mass.

Recently, considerable questions have been raised on the validity of Gibbs–Thompson equation for semicrystalline polymers. For example, recent studies by Muthukumar^{9,10} demonstrate that extended chain crystals may not be the requisite for the thermodynamically equilibrium state. Following the entropic calculations the author shows that the thermodynamically favorable structure would be the chain folded crystals where the chains are adjacently re-entrant. These findings are in accordance with the recent studies performed by Höhne¹¹ on linear polyethylene that also suggest that melting temperature will be influenced by the number of CH₂ units involved in crystal to liquid transition not the crystal stem length only. Thus, the melting temperature will strongly depend on the topological constraints that may involve more than one stem, thus greater the number of CH₂ units involved in conformational changes from trans to gauche, higher will be the melting temperature – independent of the crystal thickness. Considering these concepts Höhne

Received: June 16, 2011

Revised: September 8, 2011

Published: September 29, 2011

proposed the modified Gibbs–Thomson equation¹¹

$$T_m^n \approx T_m^\infty \left(1 - \frac{\Delta_m G_e}{\Delta_m H_{r.u.}^\infty} \frac{1}{n} \right) \quad (2)$$

Where n is the number of repeating units in the chain stem rather the crystal thickness l and G_e is total excess Gibbs free energy rather than only the surface energy, which is only part of the total excess Gibbs free energy. The number n is number of repeating units of the chain molecule, related to the crystal lamella thickness as the distance between two repeating units and the tilt angle within the crystal thickness are known.

The melting behavior and the resulting crystallization aspects have been also challenged in a series of publications reported by Strobl.^{12,13} The author shows the presence of equilibrium melting temperature much below the anticipated equilibrium melting temperature predicted from the Gibbs–Thomson equation. These observations combined with the earlier studies reported on polyethylene crystallization under pressure lead to the conclusion that polymer crystallization will always proceed via a metastable phase.¹⁴

In simple terms, crystal melting should be the reverse process of crystallization. However, in polymers such a situation complicates as the studies are often performed on aggregate of crystallites, such as spherulites. Since polymers are semicrystalline, randomization of chain during melting process is strongly influenced by morphology that it adopts during crystallization, for example whether the chain is shared between different crystals or is folded back and forth within the same crystal. Consequence to these complications and abstract topology of the chain within crystal aggregates of the spherulites, melting of spherulites as observed between cross-polars is not the shrinking process of the spherical aggregates but diffusion of the intensity suggesting random melting of the crystal aggregates.

Recently, Toda et al.¹⁵ followed crystallization and melting behavior of single crystal polyethylene. The authors crystallized single crystals in its own melt at temperatures close to the melting point. By annealing process any imperfections arising during crystallization were removed. Melting followed on the single crystal showed linear decrease in the crystal length with time invoking the inverse of crystallization as anticipated. The continuous decrease in length at fixed temperature invoked the concepts of kinetics in melting.

In parallel to these developments it is also shown that in spite of chain folded crystals nascent UHMW–PE having molecular weight greater than a million g/mol, has a melting temperature closer to the equilibrium melting point. Recent studies attribute the high melting temperature to topological restrictions that arises in the amorphous region of the nascent polyethylene. The difference in melting behavior between commercially available nascent entangled UHMW–PE and lab scale synthesized nascent “disentangled” UHMW–PE is realized by invoking kinetics.

To perform experimental studies using conventional or modulated DSC it is essential to recall studies performed by Wunderlich,¹⁶ where the author shows differences in the true and measured melting temperature of a polymer. Wunderlich et al.¹⁶ has shown heating rate dependence on peak melting temperature for different crystal morphology. For example, in case of extended chain crystal morphology where crystals cannot reorganize, the melting temperature decreases with decreasing heating rate.¹⁶ In such cases, the increase in peak melting temperature with increasing heating rate is associated with the superheating

effect.^{15,17} The increase in melting temperature includes the effect of measurement delay from the instrument.

Danley et al.¹⁸ and Toda et al.¹⁷ have shown an effective calibration method to measure true heat flow and true sample temperature by using instrumental coefficients predetermined using a standard sample, such as Indium. These authors successfully removed instrumental delays during heat flow. After instrumental correction Toda showed that in polyethylene having folded chain crystals, where crystal reorganization is feasible, melting temperature decreases with decreasing heating rate.^{15,19–24} The authors associated nonlinear dependence of melting temperature on heating rate to the entropic barrier.¹⁵ Rastogi et al. have also shown involvement of different activation barriers in melting of “disentangled” UHMW–PE with temperature and time scale. The authors showed that in nascent “disentangled” UHMW–PE, melting can occur at much lower temperature by successive detachment of the single or multiple stems from the crystal surface whereas at higher temperature melting proceeds by breakdown of the larger parts of lattice.^{8,19,20} Melting in polymer crystals depends upon the chain topology present in the amorphous phase.

Further, Toda et al.¹⁵ have successfully shown the effective use of TM–DSC in studying the melting behavior of polymer crystals by applying so-called “periodically modulating driving force”. In TM–DSC, a periodic modulation in temperature along with a linear heating or cooling is applied to examine the response of heat flow to obtain heat capacity from the modulation components of temperature and heat flow.^{25–30} The characteristic time (τ), which characterizes the pace of melting transition of each crystallite, can be calculated from the imaginary part of the effective heat capacity by,^{15,23,31–34}

$$\widetilde{\Delta C} \approx \frac{\overline{F}}{2\pi\beta\tau} \times (\text{period}) \dots \quad (3)$$

where $\widetilde{\Delta C}$ is the imaginary part of the effective heat capacity, \overline{F} is the peak height of the underlying heat flow and β is the heating rate. The characteristic time (τ) can be calculated from the slope of the linear fit of the imaginary part of the effective heat capacity to the modulation periods.

To have insight into melting process, recently, advanced experimental tools such as microchip calorimeters have been developed by Schick and co-workers.³⁵ Making use of the extraordinary high heating rates such as 30 000 K/min, where the reorganization processes in the polymers such as iPS, PET etc can be suppressed, the authors have shown that the melting occurs with the relaxation of rigid amorphous fraction just above the glass transition temperature. By using the fast heating calorimeter, these authors have also identified that by suppressing the reorganization process within the crystals, the crystals formed at the isothermal conditions melt just a few degrees above the crystallization temperature. Using TM–DSC, the influence of rigid amorphous fraction in melting behavior and consequently the organization process has been also investigated in poly(oxy-2,6-dimethyl-1,4-phenylene) by Wunderlich and co-workers.³⁶ There are several studies^{36–41} confirming the role of rigid amorphous fraction in melting process of the polymers having high characteristic ratio. However, very limited studies exist that invoke melting kinetics arising in the flexible polymer such as linear polyethylene. In this study, we use conventional DSC and TM–DSC to explore the effect of *molecular weight* and *chain topology* in amorphous phase on melting behavior of

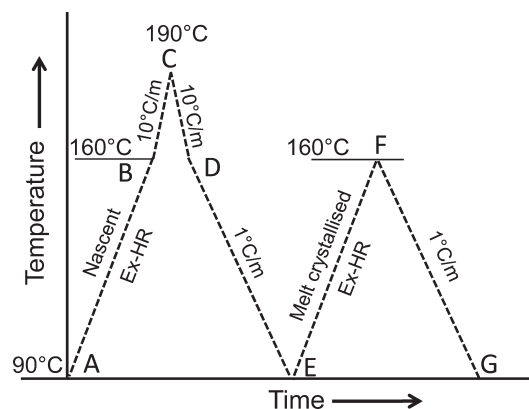


Figure 1. Schematic diagram showing the protocol for the DSC runs to study the dependence of peak melting temperature on heating rate.

nascent “disentangled”, nascent entangled and melt-crystallized samples of UHMW-PE.

MATERIALS AND EXPERIMENTAL METHODS

All the samples used in this study are “disentangled” ultra high molecular weight polyethylene (UHMW-PE) and have been synthesized using the synthesis condition described by Talebi²⁴ and Pandey et al.⁴² A commercially available grade of UHMW-PE from DSM has also been used to understand the difference in melting kinetics between synthesized “disentangled” and commercially available entangled UHMW-PEs. Different molecular weight (M_w) of “disentangled” UHMW-PE samples have been synthesized using the same catalytic system and reaction conditions except for their synthesis time. All the samples have been heated at heating rates of 0.05–10 °C/min to understand the melting kinetics. To further unravel the effects of the morphology difference between the “disentangled” and the entangled UHMW-PE polymers on the melting kinetics, annealing below the peak melting temperature ($T_M^{\beta=0.05}$) is performed for varying time.

The nascent polymers (obtained directly from reactor) are mixed with antioxidant (Irganox 1010), 0.7% by weight to prevent any oxidation over the long experiments. To have homogeneous mixing of the antioxidant with the powder, the antioxidant was first dissolved in acetone and subsequently mixed with the nascent UHMW-PE powder submerged in acetone. After mixing, the powder was dried overnight in vacuum oven at 40 °C. The dried powder is used for the studies described below.

For all the thermal characterisations, Q-2000 MDSC from TA Instruments, USA has been used. Nitrogen gas with a flow rate of 50 mL min⁻¹ is purged through the cell. High precision T-zero pans purchased from TA Instruments are used in all the tests. The nascent powder after addition of antioxidant and drying has been directly used in the pans with weight of the sample being between 1.0 and 1.05 mg. Temperature and enthalpy calibrations have been performed using indium.

EXPERIMENTAL PROTOCOLS

1. Peak Melting Temperature Dependence on Heating Rate. The following protocol has been used to study the heating rate dependence of peak melting temperature for nascent and melt-crystallized sample of the same polymer which is also schematically presented in Figure 1.

- From A to B → heating from 90 to 160 °C at examined heating rate (Ex-HR) – nascent sample.
- From B to C → heating from 160 to 190 °C at 10 °C/min.

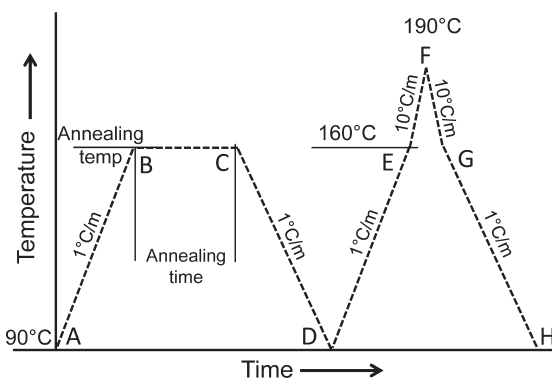


Figure 2. Schematic diagram showing the protocol for the DSC runs to study the effect of annealing on the samples below their respective $T_M^{\beta=0.05}$ temperature on the melting kinetics.

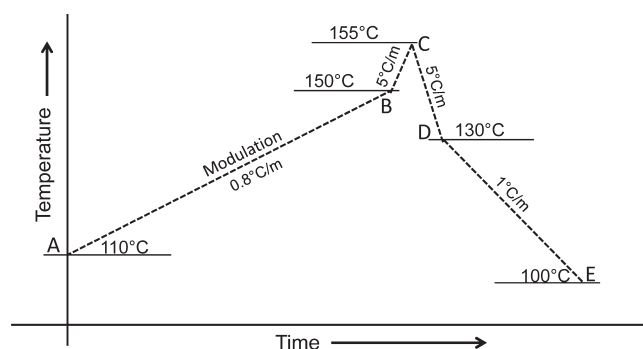


Figure 3. Schematic diagram showing the protocol for the TM-DSC runs to study the characteristic melting time of “disentangled” samples.

- From C to D → cooling from 190 to 160 °C at 10 °C/min.
- From D to E → cooling from 160 to 90 °C at 1 °C/min.
- From E to F → heating from 90 to 160 °C at examined heating rate (Ex-HR)—melt-crystallized sample.
- From F to G → cooling from 160 to 90 °C at 1 °C/min.

2. Annealing below Peak Melting Temperature ($T_M^{\beta=0.5}$) for Varying Time. The following protocol has been used to study the effect of annealing in the vicinity and below the peak melting temperature to understand melting of the crystals which is also schematically presented in Figure 2.

- From A to B → heating from 90 °C to the examined annealing temperature (T_A) at 1 °C/min.
- From B to C → annealing at the examined annealing temperature for varying time (melting in the vicinity but below the $T_M^{\beta=0.5}$) where β in superscript of T_M represents the heating rate in °C/min.
- From C to D → cooling from examined annealing temperature (T_A) to 90 at 1 °C/min.
- From D to E → heating from 90 to 160 °C at 1 °C/min.
- From E to F → heating from 160 to 190 °C at 10 °C/min.
- From F to G → cooling from 190 to 160 °C at 10 °C/min.
- From G to H → cooling from 160 to 90 °C at 1 °C/min.

3. Characteristic Melting Time (τ) by TM-DSC. The following protocol has been used to study the characteristic melting time (τ) of the crystals to understand the difference between entangled and “disentangled” samples. The protocols used are also schematically presented in Figure 3.

- From A to B → heating from 110 °C (after isothermal for 30 min) to 150 °C for the examined modulation period at heating rate of

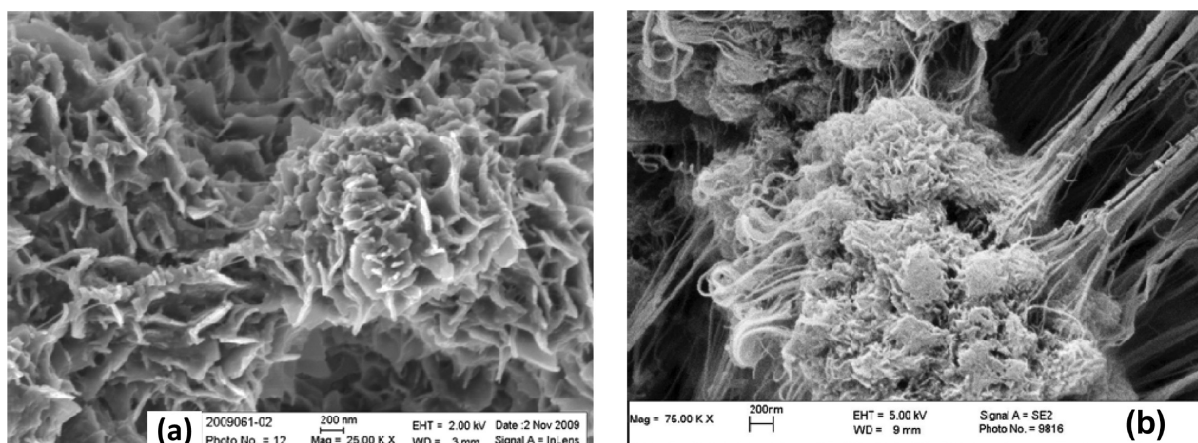


Figure 4. SEM pictures for morphology of (a) the synthesized nascent “disentangled” polymer of $M_w \sim 3$ million g/mol and (b) commercially available nascent entangled polymer of $M_w \sim 4$ million g/mol.

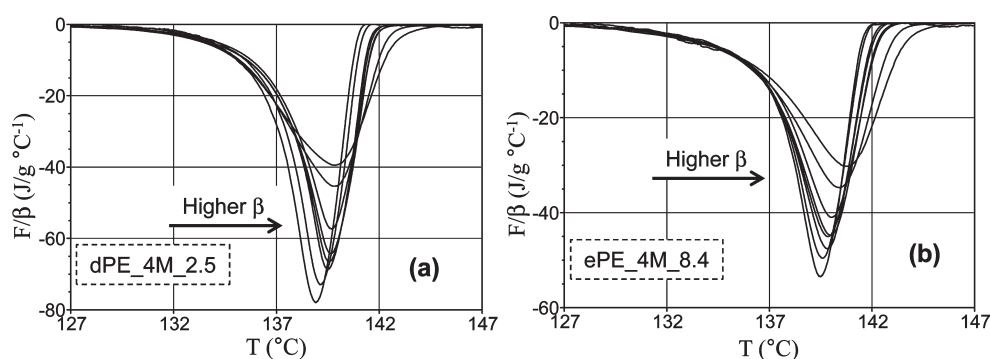


Figure 5. Endotherms at different heating rates of 0.05–10 °C/min for (a) “disentangled” and (b) entangled UHMW–PE samples of similar M_w , 4 million g/mol. F is the heat flow rate concerning the melting kinetics, where F is normalized by the heating rate (β), F/β (see ref 15). The integration of F/β over the temperature range gives the total endothermic heat, i.e., the heat of fusion. The integrated area should be independent of the heating rate. Because of melting kinetics melting region widens with the increasing heating rate, and subsequently the peak height decreases to maintain the area independent of the heating rate.

0.8 °C/min. Sinusoidal temperature modulation was used with the modulation period in the range of 10–100 s and the amplitude satisfying the heat only condition; the maximum amplitude of ± 0.2 °C was used.

- (b) From B to C \rightarrow heating from 150 to 155 °C with zero modulation at 5 °C/min.
- (c) From C to D \rightarrow cooling from 155 to 130 °C at 5 °C/min.
- (d) From D to E \rightarrow cooling from 130 to 100 °C at 1 °C/min.

SEM Investigations on morphologies of nascent reactor powders were carried out with a high resolution FEG SEM (Carl Zeiss Leo 1530 VP) operated at 5 kV. As-polymerized particles were carefully deposited on SEM stubs and the samples were coated with gold by sputtering technique.

RESULTS AND DISCUSSIONS

Figure 4 shows typical morphology of the nascent, as-synthesized, “disentangled” polymers. Randomly arranged (not stacked lamellae), single chain crystals of the order of 20 nm thickness are visible. An example of single chain forming single crystal is shown in the Supporting Information.

1. Peak Melting Temperature Dependence on Heating Rates. *a. Heating Rate Dependence of Peak Melting Temperature in Nascent “Disentangled” and Entangled UHMW–PE.* In this

study, we aim to extend our previous studies by exploring the effect of molecular weight (M_w) on the “disentangled” UHMW–PE having nonstacked single crystals. A comparison between the melting of “disentangled” and entangled UHMW–PE samples, having similar M_w , will be also pursued.

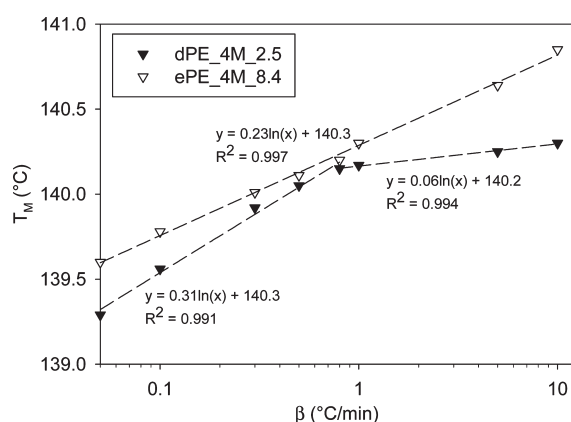
Figure 5 shows the endotherms for nascent “disentangled” (dPE_4M_2.5) and entangled (ePE_4M_8.4) samples of similar M_w at different heating rates of 0.05–10 °C/min. Heat flow at different heating rate has been normalized by respective heating rate. The increase in peak melting temperature (T_M) with increasing heating rate are in agreement with the studies performed by Toda et al.¹⁵ on polyethylene having M_w of 32 100 g/mol. All the samples listed in Table 1, investigated in this study show endotherms similar to Figure 5 where peak melting temperature increases with the increasing heating rates. Figure 6 shows the increase in peak melting temperature at different heating rates for nascent “disentangled” and entangled UHMW–PE.

In Figure 6, the heating rate dependence on melting temperature of the nascent “disentangled” and the nascent entangled UHMW–PE, having similar molecular weight, is shown. The peak melting temperature increases with increasing heating rate for both the polymers. Such an increasing trend of T_M with heating rate is reported in polymers having extended chain crystal

Table 1. Molecular Weight (M_w) and Molecular Weight Distribution (MWD) for the UHMW-PE Samples Used in the Study^a

sample	M_w ($\times 10^6$ g/mol)	MWD	$T_M^{\beta=1}$ ($^{\circ}\text{C}$)	$T_M^{\beta=0.05}$ ($^{\circ}\text{C}$)
dPE_1M_1.9	1.4	1.9	139.0	137.9
dPE_2M_2.2	2.3	2.2	139.4	138.3
dPE_4M_2.5	3.9	2.5	140.2	139.3
dPE_8M_5.2	8.1	5.2	140.8	140.4
ePE_4M_8.4	3.7	8.4	140.4	139.7

^a Peak melting temperatures ($T_M^{\beta=1}$) at the heating rate (β) of $1^{\circ}\text{C}/\text{min}$ is listed for the samples. Sample ePE_4M_8.4 is a commercially available UHMW-PE sample (entangled) from DSM whereas all other samples are synthesized “disentangled” UHMW-PE.⁴² M_w and MWD have been measured from melt rheology using the methods described elsewhere.^{42,43}

**Figure 6.** Heating rate comparison between synthesized nascent “disentangled” (dPE_4M_2.5) and commercially available entangled (ePE_4M_8.4) UHMW-PE of similar M_w .

morphology, where crystal thickening/perfectioning cannot occur.¹⁶ Contrary to the extended chain crystals, in the polymers where crystal thickening/perfection can occur by reorganization T_M increases with decreasing heating rate. All the synthesized “disentangled” UHMW-PE samples used in this study possess folded chain morphology where crystal thickening/perfection by reorganization should be feasible.^{20,21,44} However, in the folded chain morphology the crystal thickening/perfectioning during heating requires larger co-operative motion of the chains within the crystals of $M_w > 1 \times 10^6$ g/mol, and will be a relatively slow process compared to melting.

The increase in T_M with heating rate is attributed to the superheating effect, where the measured melting temperature is higher than the true melting temperature of the crystal. Wunderlich and co-workers¹⁶ explained the main cause of superheating in DSC measurement to thermal lag between the heat source and the sample, i.e. measurement lag between the true sample temperatures and melting of crystals. The apparent shift in peak melting temperature caused by instrumental delays cannot be corrected alone by temperature calibration using the onset melting temperature of standard materials (such as indium) at the respective heating rates.¹⁷ Schawe⁴⁵ has shown that the shift in peak melting temperature depends upon peak height and the slope of heat flow. To circumvent these artifacts TA Instruments has introduced a new method of measuring heat flow in their

selective instruments (such as MDSC-Q2000 used in this study) with aim to improve the measurement by including the heat storage effects of sensor and the pans. A new calibration procedure is used to determine the instrument coefficient which is used to obtain actual heat flow in the sample.¹⁸ Toda et al.^{15,17} have used this method described in ref 17 for examining the heating rate dependence on the peak melting temperature. To avoid any reorganization these authors annealed polymer crystals for several hours prior to the experiments. In spite of the instrumental corrections, Toda et al. observed increase in melting temperature with heating rate in various polymers PP, PE, PET, and PVDF.^{15,17} The authors found nonlinear dependence in melting of the single crystals of linear polyethylene. Their observations were supported by microscopy studies.

A nonlinear logarithmic dependence of increasing peak melting temperature on heating rate for nascent “disentangled” and entangled polymer is evident from Figure 6. Peak melting temperature increases as a function of the logarithm of heating rate for both, “disentangled” and entangled polymers having similar M_w . Contrary to the single heating rate dependence for the entangled polymer two distinct heating rate dependence of peak melting temperature for the synthesized “disentangled” polymer exists, Figure 6.

It is to be noted that in the entangled polyethylene, ePE_4M_8.4, with the increasing heating rate low-temperature sections of the curves shifts to the higher temperature so is the peak melting temperature (Figure 5b). The shift in the melting temperature follows the logarithmic increase with the heating rate (Figure 6). Unlike the entangled sample, the “disentangled” polyethylene dPE_4M_2.5 shows shift in the low temperature section to the high temperature while increasing the heating rates from 0.05 to $1.0^{\circ}\text{C}/\text{min}$. Above this heating rate, from 1.0 to $10.0^{\circ}\text{C}/\text{min}$, the lower temperature section of the curve shifts to lower values. The change in the direction of the low temperature section of the curve in the region of $1.0^{\circ}\text{C}/\text{min}$ is a phenomenon observed for all the nascent “disentangled” polyethylene samples that show change in the peak melting temperature slope with heating rate at $1.0^{\circ}\text{C}/\text{min}$ (for example Figure 6 and more information on the molecular weights are shown in the Supporting Information).

What follows is a possible explanation of the distinct difference in melting behavior of the entangled and the “disentangled” crystals. In the nascent “disentangled” crystals the appearance of two different slopes with heating rate strongly suggests presence of two different mechanisms involved in the melting process. At the heating rates greater than $1^{\circ}\text{C}/\text{min}$, melting should be a normal process where it would proceed in clusters of chain stems. Above $1^{\circ}\text{C}/\text{min}$, the slope in Figure 6 suggests stronger heating rate dependence of the nascent entangled sample compared to the nascent “disentangled” polymer. From the modified Gibbs–Thomson equation (see eq 2), at the fixed heating rate, higher melting temperature of entangled nascent crystals compared to “disentangled” nascent crystals means detachment of greater number of methylene units from the entangled nascent crystals. The difference in nonlinear melting temperature variation on heating rate in the two samples invokes melting kinetics, whereas the difference in slopes of the two samples shown in Figure 6 should be correlated with the topological differences that exist in the amorphous component of the two semicrystalline polymers. The change in slopes arising due to topological differences has been discussed further in more detail.

However, at the heating rate lower than $1^{\circ}\text{C}/\text{min}$, in the nascent “disentangled” sample (Figure 6) sudden increase in T_M slope with the heating rate is observed. The sudden change in slope

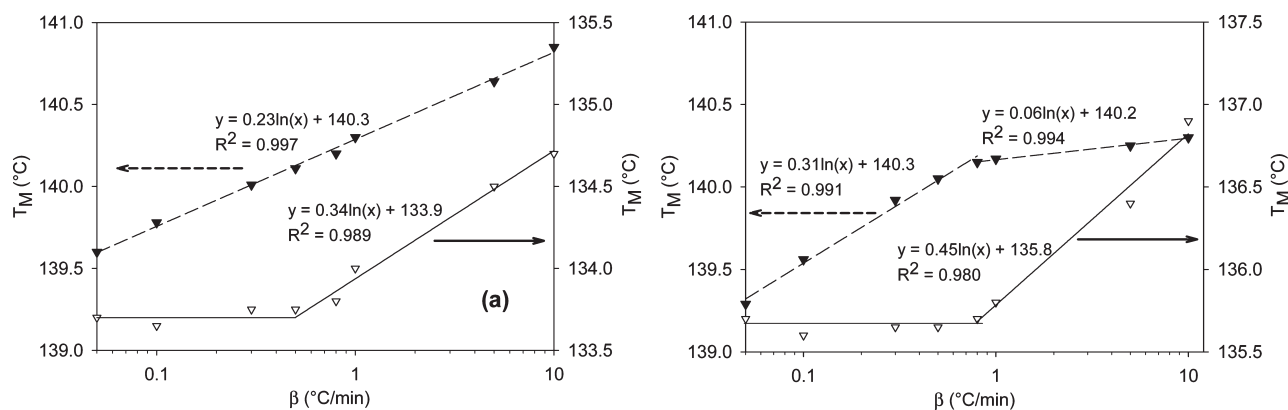


Figure 7. Peak melting temperature dependence on heating rate between nascent crystal (filled symbols) and melt-crystallized (open symbols) of (a) the entangled, ePE_4M_8.4 and (b) the “disentangled” UHMW-PE, dPE_4M_2.5, of similar M_w .

suggests involvement of different activation barrier in the melting process. Here we recall some of the earlier findings reported by us where we showed differences in the enthalpic activation barrier for detachment of chains either via cluster melting or consecutive detachment of chain stems from the crystal surface, followed by their diffusion in surrounding melt.¹⁹ Considering these concepts an explanation for the two different mechanisms involved in the melting process of the “disentangled” nascent polymer could be provided. At the heating rates below 1 °C/min, where the system is given sufficient time for chain detachment process, melting in the nascent UHMW-PE polymers is likely to start from the outer surface by consecutive detachment of chain stems. Melting from the outer surface compared to the core of the crystal would be preferred due to lower surface free energy requirement, i.e., lower entropic barrier for the chain segments in contact with melt. The number of chain stems involved in melting decreases with decreasing heating rate, so is the melting temperature. On increasing the temperature sufficiently high, i.e., increasing heating rate above 1 °C/min the difference in surface free energy requirement for chain detachment from the crystal surface or from center is suppressed, thus a new activation barrier is overcome that does not require consecutive melting and overcomes the entropic barrier to an extent that nucleation process for melting can occur at different places of the crystal.

In the case of nascent entangled polymer, melting can occur only in clusters as chains are shared among many crystallites and larger co-operative motion is required to achieve the random coil state. For the same heating rate, higher T_M of the entangled polymer compared to the “disentangled” polymer, also supports the requisite for larger co-operative motion in melting of the nascent entangled polymer. The increase in T_M with increasing heating rate corresponds to the cluster size involved in the melting process, which increases with the increasing heating rate.

Higher heating rate dependence of the entangled polymer compared to the “disentangled” polymer, at the heating rates >1 °C/min, is due to the presence of greater number of entanglement in the amorphous region of the nascent entangled sample. From Figure 6, it is evident that distinction occurs in melting behavior of the entangled and the “disentangled” samples. Considering that the crystallinity and crystal structures of the two polymers is the same the arising differences in the melting behavior should be dependent on the topological differences residing in the amorphous regions, thus invoking kinetics in melting process of the semicrystalline polymers.

One of the methods to probe differences in the amorphous regions is solid-state NMR. The ^{13}C -single pulse magic angle spin studies (SP-MAS) performed on these samples confirm distinction between the amorphous chain segments; for example, entanglement in the entangled sample hinders the chain diffusion process from the amorphous to the crystalline region.^{46–48} In consequence, the transfer of polarization to the crystalline region takes a longer time in the entangled sample compared with the “disentangled” polymer.⁴⁹ A further major distinction is encountered when segmental mobility in the amorphous region is considerably enhanced in the melt-crystallized samples compared to the nascent polymers.⁴⁶ The entropic differences that arise between the amorphous and the crystalline regions, due to enhanced segmental mobility of the amorphous region, stops the chain diffusion process between the two regions below the α relaxation temperature of the melt-crystallized sample.

To investigate the influence of topological differences in the melting process, what follows is a comparative study on the heating rate dependence of the nascent and its melt-crystallized samples.

b. Heating Rate Dependence on Melting Temperature of the Nascent and Melt-Crystallized Polymer. Figure 7 presents the heating rate dependence of the nascent and the melt-crystallized samples of the same polymer. The melt-crystallized sample is obtained on melting of the nascent crystals to 190 °C during first heating step (step 1a, Figure 1) of the DSC run and recrystallizing by cooling at 1 °C/min from its melt to 100 °C (step 1d, Figure 1). Data from the first heating step is treated as melting of nascent crystals, whereas the second melting represents data on melt-crystallized of the same sample (step 1e, Figure 1), thus avoiding any complication caused by difference in molecular characteristics of the samples. A clear difference in heating rate dependence and melting temperature between the nascent crystals and the melt-crystallized samples is apparent from Figure 7. The peak melting temperature of the melt-crystallized sample is lower than the nascent crystals of the same polymer at any examined heating rate. Peak melting temperatures of 133.7 and 135.7 °C at slower heating rates (<1 °C/min) for melt-crystallized of entangled and “disentangled” polymer, respectively, are close to the peak melting temperature of 131 °C predicted by the Gibbs–Thomson equation for polyethylene with the lamellar thickness of 25 nm.⁷ However, the higher peak melting temperature of ~ 140 °C for the nascent samples having chain folded crystals, which is close to the equilibrium melting

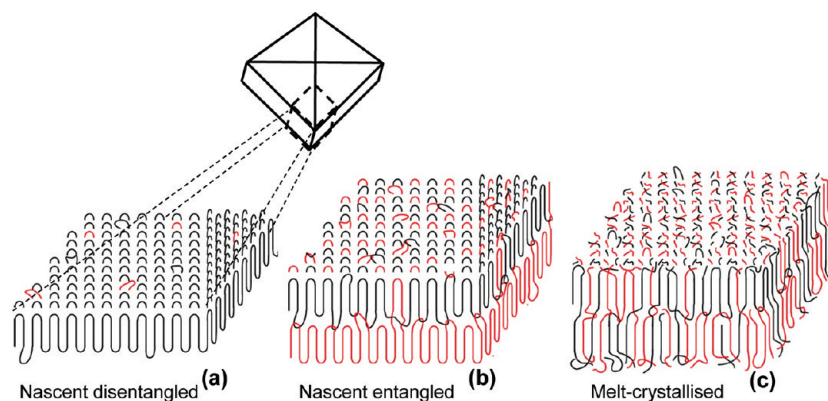


Figure 8. Schematic representation of the crystals structure for (a) nascent “disentangled” sample having re-entry chains with tight folds, (b) nascent entangled sample having tight folds with re-entry with chains shared among several crystals, and (c) melt-crystallized sample having loose chain folds and loops with chains being shared among several crystals. To have the schematics of nascent “disentangled” sample in agreement with Figure 4a that represent a single crystal like morphology, a scenario of single chain forming single crystal is depicted. However, the sporadic occasions where a chain can be shared between different crystals cannot be ignored and such a possibility is shown by red folds on the crystal surface.

temperature of 141.5 °C for polyethylene having extended chain crystals, cannot be explained by the Gibbs–Thomson equation.⁸ Engelen et al.⁴⁴ have reported that nascent crystals are folded chain crystals which on cross-linking by irradiation show a low melting temperature of ~135 °C. Using DSC and NMR, we have attributed the high peak melting temperature of nascent crystals to crystal topology.²⁰ The topological differences in amorphous phase of the crystals have profound effect on melting of the polymer. Höhne¹¹ has shown the number of repeating units involved in the melting dynamics governs the melting rather than the thickness of the lamella and the surface energy.

To explain differences in the heating rate dependence on the melting temperature of the melt-crystallized sample and the nascent polymers, in Figure 8 we show schematic illustration of the crystal structure for nascent entangled, nascent “disentangled” and melt-crystallized samples. In a nascent entangled sample that is polymerized at high temperatures using a Z–N supported catalytic system, having highly active sites close to each other, the crystals comprise the same chain that also participates in formation of several other crystallites. The amorphous region between the crystals comprises of amorphous region having tight chains without having any specific crystallographic registration. The presence of tight chains in the amorphous region is supported by the solid state NMR studies.^{20,47,48}

In the case of nascent “disentangled” sample, crystals are mainly formed by re-entrant chains, ultimately monomolecular crystal, where most of the chains do not participate in formation of other crystallites; i.e., the single-site catalytic system combined with low polymerization temperature and low catalyst concentration promotes such a possibility. The existence of tight folds, leading to restricted chain mobility of the chain segments in the amorphous region becomes apparent from the solid state NMR studies. To recall single pulse NMR studies also support the topological differences in the entangled and the “disentangled” nascent polymers.^{20,47,48}

In melt-crystallized samples of these ultrahigh molecular weight polymers, chains are most likely to participate in the formation of several crystals with least adjacent re-entry. The presence of highly mobile chain segments in the amorphous region revealed by the NMR studies confirm the presence of loose chain folds or loose chain segments and higher conformational or

entropic differences between the amorphous and the crystalline regions.⁴⁸ This entropic difference means that the detachment of chain segment from the crystal surface is not dependent on the neighboring chain or the presence of the part of chain in the other crystal. In summary, when given sufficient time (low heating rate) the chain detachment process from the crystal surface will be equal to the crystal thickness obeying the Gibbs–Thomson equation. Such a possibility is apparent from the plateau region observed for the melt-crystallized samples in Figure 7. However, at the higher heating rates, melting temperature increases with the heating rate. The cause for the increase in the melting temperature is attributed to the simultaneous cooperative detachment of chain segments from the crystals and its neighbors. The number of methylene units detached from the crystal tends to increase with the increasing heating rate, thus causing an increase in the melting temperature.

In the melt-crystallized sample, the independence of melting temperature on the heating rate below a critical value strengthens the argument that no correlations between the neighboring chains that are connected by the amorphous region, within the crystals exist. Sudden change in the slope with the heating rate also invokes the argument of two different mechanisms involved in melting of the melt-crystallized sample. The difference in mechanisms is encountered when the melting zones with decreasing heating rate shrink to chain segments corresponding to crystal thickness. Since the chain segments at the crystal surface does not feel the presence of its neighbor or its connectivity to the chain segment residing within the neighboring crystal, melting temperature shows heating rate independence; a situation in contrast with the “disentangled” and entangled nascent samples.

It is important to realize that because of the very nature of polymer synthesis, at least in the initial stages, the commercial polymer will have much higher number of entanglement in its melt state compared to the melt of the synthesized “disentangled” polymer. The difference in the entanglement in the melt state will have implications on the crystallization behavior. To recall, a “disentangled” polymer upon melting goes from a “disentangled” to an entangled state where the time required to attain the thermodynamically stable entangled state follows the power law of 2.6 to the molecular weight.^{21,24,42} Considering this power law,

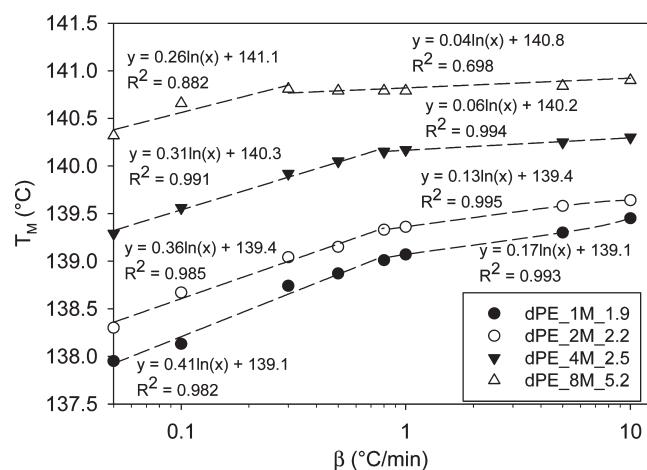


Figure 9. Heating rate dependence of “disentangled” UHMW-PE of different M_w for heating rates of 0.05, 0.1, 0.3, 0.5, 0.8, 1.0, 5.0, and 10.0 °C/min. The heating rate where the slope changes arises due to change in melting mechanism from cluster to chain detachment, which would strongly depend on the entanglement state in the amorphous region of the nascent sample.

the total time required for the sample having molecular weight 4 M will be nearly 30 h, contrary to the few minutes required in the case of the entangled commercial sample. For the sake of consistency, similar to the melt-crystallized entangled commercial sample, following the pathway depicted in Figure 1, the melt-crystallized sample of the “disentangled” nascent polymer reported in this study was also left in melt for 5 min prior to crystallization. It is documented that crystallization is facilitated from the “disentangled” melt; i.e., the onset of crystallization from the “disentangled” polymer melt is at a higher temperature compared to its entangled melt state.⁵⁰ Higher crystallization temperature also means higher crystal thickness. Thus, the difference in melting temperatures at slower heating rates, below 1 °C/min, of the melt-crystallized samples (Figure 7, parts a and b) may be attributed to crystal thickness. In Figure 7, a comparison between the slopes at higher heating rate dependence (heating rate >1 °C/min), in the nascent and its melt-crystallized sample, is observed in the melting temperature of the melt-crystallized sample. This means that by increasing the heating rate greater amount of methylene units are detached from the melt crystallized sample compared to its nascent state. Considering the morphological differences, the rate of methylene units detachment with the heating rate is likely to be influenced by two factors: (a) the number of entanglement present in the amorphous phase and (b) the number of chains participating in formation of several other crystallites. Compared to the nascent “disentangled” sample, chains participating in the neighboring crystals will be higher in the nascent entangled sample; thus, the melting temperature dependence on the heating rate will be higher in the nascent entangled sample.

c. Heating Rate Dependence for “Disentangled” Polymers Having Different M_w s. Figure 9 shows the nonlinear logarithmic heating rate dependence in the “disentangled” polymers having different M_w . It is apparent that all the polymers show discrete change in the melting temperature above a “critical” heating rate, thus dividing melting temperature into two regimes low (heating rate <1 °C/min) and high (heating rate >1 °C/min). Second, it is evident that melting temperature at a fixed heating rate increases

with increasing molecular weight. The increase in melting temperature suggests detachment of increasing number of methylene units with increasing molecular weight. A possible explanation of this is the topological requirement that the higher molecular weight imposes, that may arise due to adjacent re-entry and/or presence of lesser number of entanglements in the amorphous region. Recently, by combining the polymerization conditions with the rheological studies we have demonstrated decrease in the entanglement density with increasing molecular weight.⁴²

From the Figure 9, it is also evident that at low heating rates, melting temperature increases faster with the heating rate in the low molecular weight polyethylene. Following the concepts described in the section above, the difference in the melting temperature with the heating rate is in cohort with the differences in the entanglement density of the low and the high molecular weight nascent “disentangled” polyethylene.

From the results summarized above, it is conclusively shown that heating rate has a strong dependence on the melting behavior that is associated with the topological constraints. In Figure 9, the experiments are performed to the lowest accessible heating rate of 0.05 °C/min. To have further insight into the melting kinetics, that is influence by the topological constraints present in the amorphous component of the semicrystalline polymer, in the following section studies are performed at fixed temperature below the peak melting temperature, for $\beta = 0.05$ °C/min.

2. Melting Behavior in the Vicinity of Peak Melting Temperature. *a. Annealing of Nascent Entangled and “Disentangled” Samples below the Peak Melting Temperature (T_A).* Figure 10 compares DSC thermograms obtained at heating rate of 1 °C/min, for a nascent “disentangled” sample dPE_2M_2.2, after annealing it at various temperatures (T_A) and times in the vicinity but below the peak melting temperature determined for the heating rate of 0.05 °C/min ($T_M^{\beta=0.05}$). Figure 10 shows appearance of a second melting peak at lower temperature (T_{M1}) that grows with the increasing annealing time and temperature. With the increasing prominence of lower melting peak (T_{M1}) at higher annealing temperature and time, the higher melting peak (T_{M2}) decreases in magnitude, Figure 10. Considering position of the peaks, the low melting peak is associated with melting of the melt crystallized polymer obtained on annealing, whereas the high melting peak is correlated with the remainder of crystal that has not molten on annealing. The increase in magnitude of the low melting peak with annealing time suggests the involvement of kinetics in the melting process arising due to morphological restrictions that the nascent “disentangled” polymer imposes. These observations are in accordance with our earlier studies^{8,19–21} where the kinetics involved suggests successive detachment of chains from the crystal surface and its reeling into melt. The shift in high temperature melting peak with annealing time suggests an ongoing reorganization process in the remainder of the crystals.

The area under the two peaks is calculated as labeled in Figure 10d. To provide some quantitative estimation on the amount of crystal melted during the annealing process, percentage ratio of the area A2 (area under the lower peak) to the total area (area A1 + area A2) is taken as a measure at different annealing conditions. Figure 10d also compares the difference between melting of a nascent “disentangled” sample, before and after annealing at ($T_M^{\beta=0.05} - 0.3$) °C for 30 min. The decrease in total enthalpy (summation of ΔH for T_{M1} and T_{M2}) in the annealed sample, compared to the nascent sample, arises due to loss in crystallinity in the melt-crystallized component of the polymer.

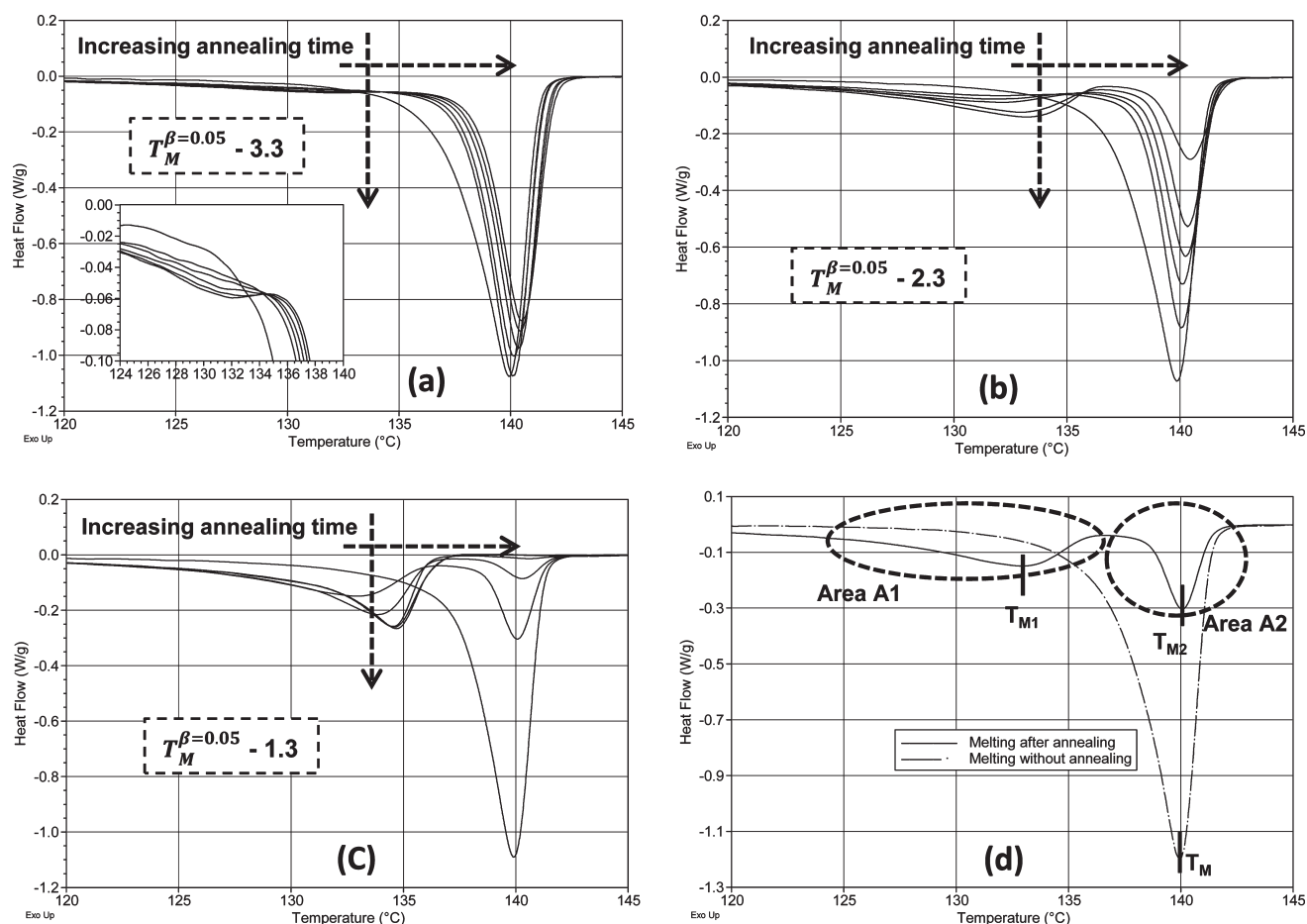


Figure 10. Second heating step for the nascent “disentangled” samples dPE_4M_2.5 after annealing at (a) ($T_M^{\beta=0.05} - 3.3$) °C, (b) ($T_M^{\beta=0.05} - 2.3$) °C and (c) ($T_M^{\beta=0.05} - 1.3$) °C for different times (0, 30, 60, 90, 120, 240, and 480 min). With increasing annealing times and temperatures, a lower secondary melting peak can be seen to be evolving. For annealing at ($T_M^{\beta=0.05} - 3.3$) °C, these lower peaks are small and are shown in inset. (d) Endotherms for a nascent “disentangled” sample dPE_2M_2.2 without any prior annealing and after annealing at ($T_M^{\beta=0.05} - 0.3$) °C for 30 min.

As is evident from Figure 10, the first melting peak increases in intensity faster with the increasing annealing temperature (T_A), suggesting a faster melting process, i.e., faster detachment of chains and their reeling in the surrounding polymer melt. Faster melting means lesser annealing time for the remainder of the crystal thus lesser possibility for organization, and the resultant shift in the high melting temperature. On the other hand at lower annealing temperatures, where T_A is much below the $T_M^{\beta=0.05}$ melting of the nascent crystals is not realized. Considering that the melting behavior will be strongly dependent on the molecular weight, i.e., polymerization time and the resultant entangled state⁴² for further comparison we have chosen ($T_M^{\beta=0.05} - 2$) °C as the fixed annealing temperature for the respective polymers, where $T_M^{\beta=0.05}$ is the intrinsic physical parameter for the investigated polymers.

Figure 11 shows a percentage decrease in the enthalpic area A2 (area A2 divided by the total area A1 + A2), for the nascent “disentangled” and the entangled samples having similar molecular weights (M_w), with varying annealing time at respective annealing temperature defined by ($T_M^{\beta=0.05} - 2$) °C. From Figure 11, it is apparent that A2 decreases rapidly for the nascent “disentangled” polymer, whereas, the decrease is considerably less for the nascent entangled sample ePE_4M_8.4. Similar observations have been reported earlier by us on “disentangled”

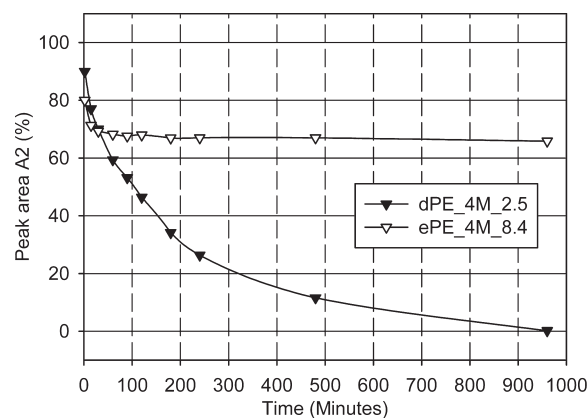


Figure 11. shows decrease in the area A2 for the nascent synthesized “disentangled” (dPE_4M_2.5) and commercially available entangled sample (ePE_4M_8.4) of similar M_w after annealing at respective temperature ($T_M^{\beta=0.05} - 2$) °C for varying times.

UHMW-PE polymers, where it is concluded that the continuous melting of nascent “disentangled” polymer proceeds by successive detachment of chain stems and their reeling into polymer melt, where the number of chain stems detached from

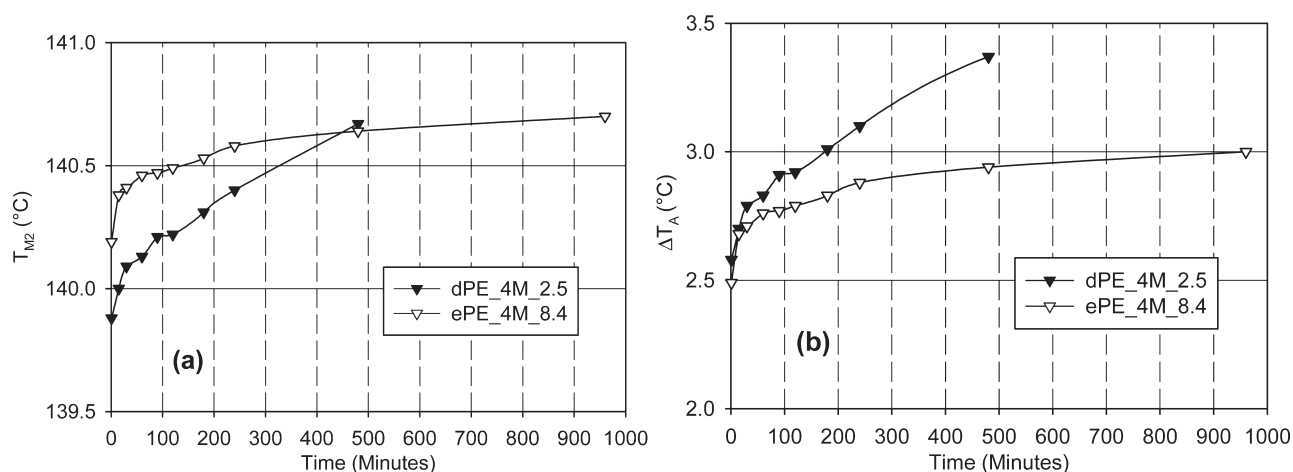


Figure 12. Increase in (a) peak melting temperature of the remainder of nascent sample, T_{M2} and (b) the difference between T_{M2} and respective $(T_M^{\beta=0.05} - 2)^\circ\text{C}$, ΔT_A , for synthesized nascent “disentangled” (closed symbols) and commercially available entangled UHMW-PE (open symbols) samples at different annealing times.

the crystal surface are strongly dependent on the annealing temperature.^{8,19,20} However, in the case of nascent entangled polymer no appreciable decrease in the area A2 on annealing suggests that melting by chain detachment does not occur. This is also confirmed by our earlier observation with heating rate dependence of the nascent entangled polymer. The strong difference in melting kinetics on annealing suggests influence of chain topology on the detachment of chains from the crystal surface. Considering melting to be the reverse process of crystallization, in normal circumstances where the chains are adjacently re-entrant melting should occur by simple successive detachment of chains. However, in the scenario where the chains are not adjacently re-entrant melting will be a more complicated process where successive chain detachment would be hindered by topological constraints residing in the amorphous component of the semicrystalline polymer. Melting behavior summarized in Figure 11 suggests differences in the topological constraints of the entangled and the “disentangled” nascent polyethylene. Recently Toda et al.¹⁵ followed melting behavior of the low molecular weight single crystal polyethylene. They conclusively showed that melting in the single crystal occurs by shrinking in crystal size, a reverse process of crystallization. These findings are in contradiction with the observed decrease in intensity on melting of spherulites rather their contraction in size. The loss in intensity is correlated with the sporadic melting process in the crystal aggregates where the chains are shared between different crystals.

In single crystals where chains are anticipated to have adjacent re-entry, decrease in crystal size should be linear. In the nascent “disentangled” samples deviation in the linear behavior with time arises due to shift in the melting temperature of the remainder of the crystal due to crystal perfectioning (Figure 12). The shift causes increase in the difference between melting and annealing temperatures thus making chain detachment process more difficult, consequently suppressing the melting rate. Hence, the rate of the melting of the nascent crystals reduces with the increasing annealing time as the measure of effective degree of superheating increases which is characterized by

$$\Delta T_A = T_{M2} - T_A \dots \quad (4)$$

where ΔT_A is the “measure” of the effective degree of superheating, T_{M2} is the peak melting temperature in second heating

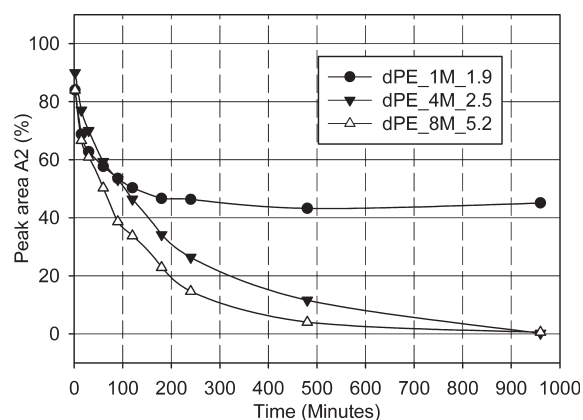


Figure 13. Decrease in the area A2 of different nascent “disentangled” polyethylene having different molecular weight. The samples were annealed at their respective $(T_M^{\beta=0.05} - 2)^\circ\text{C}$ for different time.

step (Figure 10d) after annealing at T_A for varying times, and T_A is the annealing temperature, which is $(T_M^{\beta=0.05} - 2)^\circ\text{C}$ in this study.

The nonlinearity in the decrease of area A2 with the increasing annealing time is the coupled effect of simultaneous crystal melting and crystal perfection during the annealing. As T_{M2} increases with the annealing time, Figure 12, the measure of effective degree of superheating (ΔT_A) increases at a fixed T_A causing decrease in the rate of the nascent crystal melting. Figure 12b, shows that even though the observed changes in degree of superheating with annealing time are lower in the nascent entangled sample, no decrease in the area A2 is observed (Figure 11).

b. Effect of M_w on Annealing of Nascent “Disentangled” Polymer, below Peak Melting Temperature ($T_M^{\beta=0.05}$). From the data comprised in the figures above, it is apparent that the melting rate in “disentangled” polyethylene is strongly influenced by the difference in melting and annealing temperatures ΔT_A , i.e., the lower the difference, the faster will be the melting rate, Figure 10. The possible cause of nonlinearity in the peak area A2, with increasing annealing time, is correlated with the shift in the melting temperature to higher values with annealing time, Figure 12. As a consequence to the shift, the difference between the new melting and the annealing temperature increases, ΔT_A resulting

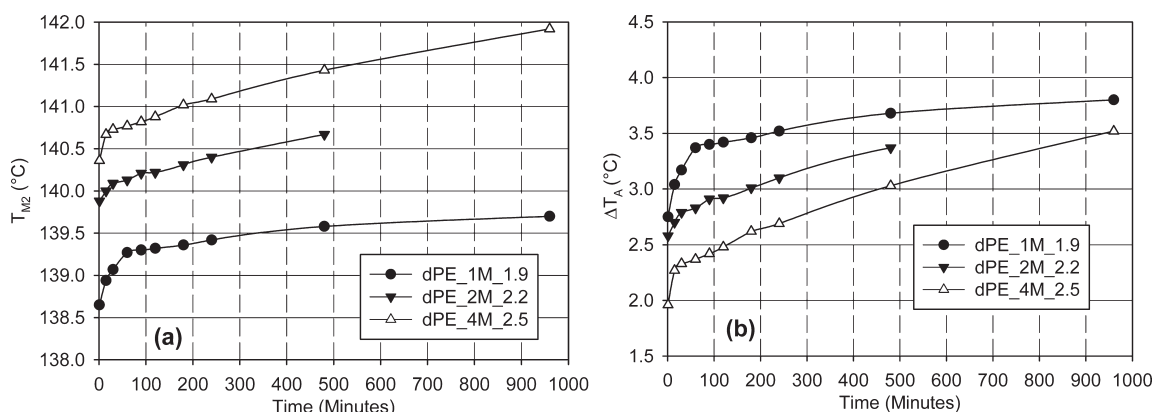


Figure 14. Increase in (a) peak melting temperature of the remainder of nascent sample, T_{M2} and (b) difference between T_{M2} and respective $(T_M^{\beta=0.05} - 2)^\circ\text{C}$, ΔT_A , with annealing time of nascent “disentangled” UHMW-PE having different molecular weights.

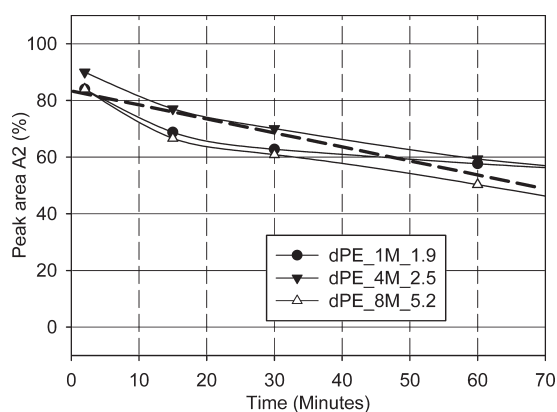


Figure 15. Decrease in the area A2 of different nascent “disentangled” polyethylenes having different molecular weights for lower annealing times (<60 min) at $(T_M^{\beta=0.05} - 2)^\circ\text{C}$.

into continuous decrease in the rate of melting and thus the nonlinearity. What follows is a study on the influence of molecular weight on melting process in “disentangled” polyethylene.

Figure 13 shows melting of nascent “disentangled” crystals at $(T_M^{\beta=0.05} - 2)^\circ\text{C}$ for different molecular weight samples, where $T_M^{\beta=0.05}$ is the intrinsic peak melting temperature of the chosen polymers at heating rate $0.05^\circ\text{C}/\text{min}$, as shown in Table 1. The figure shows that not only does melting proceed nonlinearly with annealing time but also the melting rate of the low M_w sample is the slowest and a substantial amount of the polymer does not melt. The slowest melting rate being for the lowest M_w sample appears to be counterintuitive; however, the cause becomes apparent from Figure 14b, which shows the highest increase in the measure of effective degree of superheating, ΔT_A . Contrary to the low molecular weight polymer, the high M_w sample melts fastest and shows lowest increase in the degree of superheating, Figure 13. It becomes apparent that reorganization during melting (annealing) has an important role which governs melting rate of the nascent “disentangled” crystals. Though all M_w samples have been annealed at $(T_M^{\beta=0.05} - 2)^\circ\text{C}$, the fastest increases in degree of superheating in the lowest M_w sample suggest a fast crystal perfectioning/thickening by reorganization. The faster reorganization in low M_w sample is associated with easier and faster co-operative motions in smaller crystallites. Also, as the melting proceeds from side surface, causing

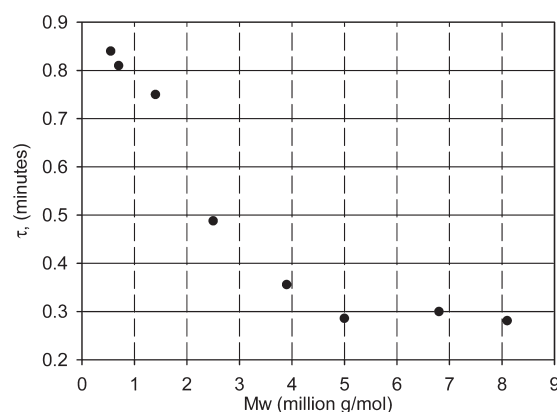


Figure 16. Characteristic melting time, τ , for the nascent “disentangled” polymers of different molecular weights. The higher the characteristic melting time, the slower will be the melting rate. The difference in characteristic time is attributed to entanglement residing in the amorphous region of the polymer.

Table 2. M_w , MWD, and Characteristic Times for Nascent “Disentangled” Polymers of Different Molecular Weights

sample	M_w (million g/mol)	MWD	τ (min) (first melting)
1	0.6	1.6	0.84
2	0.7	1.7	0.81
3	1.4	1.9	0.75
4	2.5	2.2	0.49
5	3.9	2.5	0.36
6	5.0	2.4	0.29
7	6.8	2.4	0.30
8	8.1	5.2	0.28

shrinkage of the crystal size, the crystal becomes thicker toward the center.

To avoid the effect of crystal perfectioning/thickening on melting, Toda et al.¹⁵ annealed the single crystals for considerable time. The authors conclusively showed linear decrease in crystal length with increasing annealing time. In the nascent “disentangled” polyethylene, investigated in this publication, crystal perfectioning/thickening could not be decoupled with the simultaneous melting process. However, linear decrease in

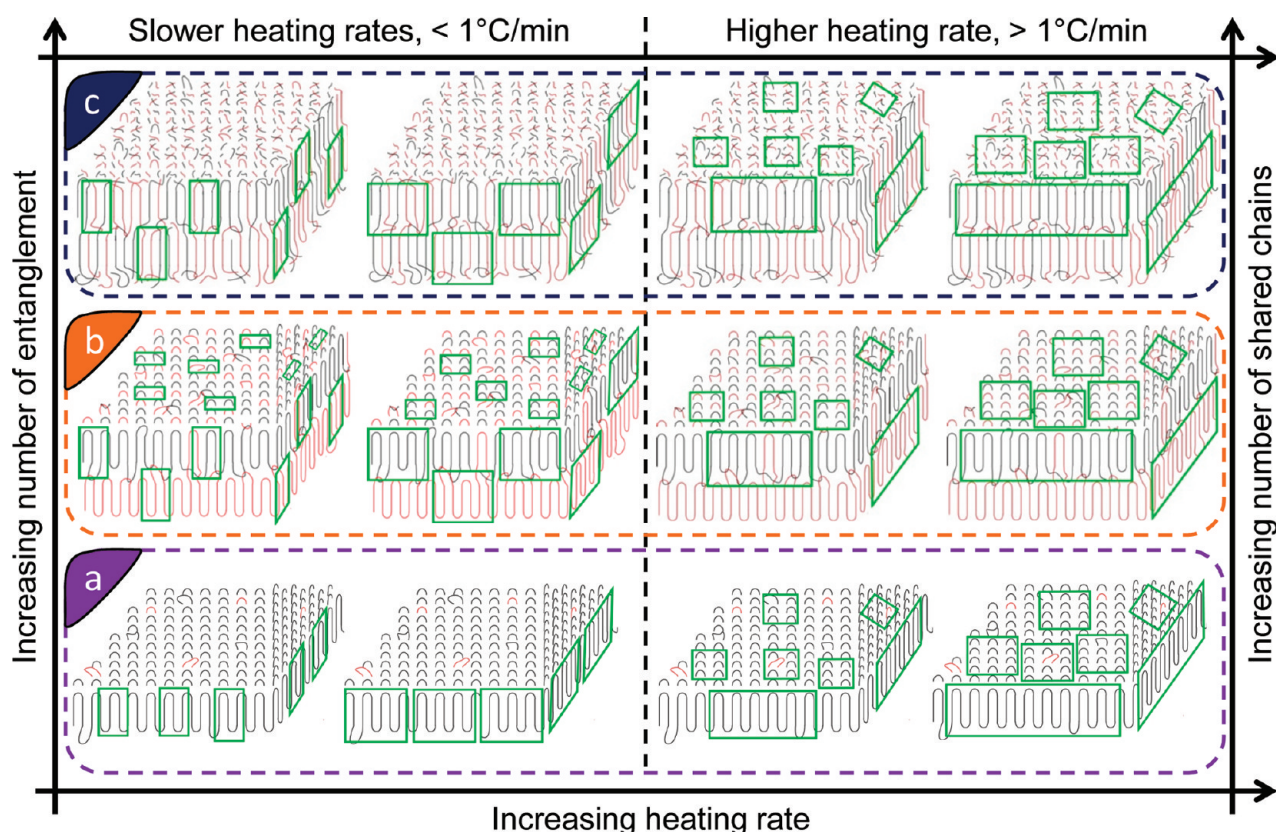


Figure 17. Schematic representation of melting at different heating rates for (a) nascent “disentangled”, (b) nascent entangled, and (c) melt-crystallized morphology. Figure also shows the increasing number of entanglement in the amorphous phase of the crystals and number of chains shared in formation of several crystallites which will affect the peak melting temperature and heating rate dependence.

melting temperature at shorter annealing times (<60 min), Figure 15, is in accordance with the observations reported on single crystals by Toda et al. The parallels in melting between single crystals and nascent “disentangled” polymer reinforces the concept of successive chain detachment and their diffusion in the polymer melt. The nonlinearity in melting can be corrected by considering the dynamics involved in the shift of ΔT_A with annealing time. However, such a correction is not feasible in nascent “disentangled” polyethylene as the melting process is coupled with the crystal perfectioning at the chosen annealing temperature.

The findings reported above by conventional DSC are further strengthened by modulated DSC. TM–DSC studies are performed to observe the effect of molecular weight on melting rate of the nascent “disentangled” UHMW–PE.

3. Characteristic Melting Time of Nascent “Disentangled” Crystals by TM–DSC. Characteristic melting time, τ , as defined in eq 3, has been calculated for nascent “disentangled” samples at the heating rate of 0.8 °C/min. Figure 16 and Table 2 shows the characteristic melting times for nascent “disentangled” polymers with different M_w . The characteristic melting time decreases with the increasing molecular weight. Lower characteristic time, for the higher M_w sample, is associated with the faster solid to liquid transition of the crystals. Thus, results summarized in Figure 16 suggests that high molecular weight polymer, having lowest characteristic time, will melt faster than the low molecular weight polyethylene. Considering that the melting in TM–DSC is followed from the peak melting temperature, the difference in melting rates for the

low and the high molecular weight may be correlated to the entangled state of the polymer, i.e., the higher entanglement density in the low molecular weight polyethylene suppresses the melting rate. These observations are in accordance with the experimental data shown in Figure 9, where higher slope of melting temperature with heating rate, in the low molecular weight polyethylene, is attributed to the greater number of entanglement residing in the amorphous region of the semicrystalline polymer. The presence of greater number of entanglement in low molecular weight polyethylene compared to the high molecular weight is also in accordance with our recent studies reported in ref 42.

CONCLUSIONS

One of the salient conclusions from the study is that melting of crystalline component in the semicrystalline polymer is not only dependent on the crystal thickness but also on topological constraints residing in the amorphous region of the polymer. This finding having implications in melting of polymers, in general, has been strengthened by making judicious choice of a series of “disentangled” polyethylene with varying molecular weight, where except the polymerization time, other polymerization conditions such as catalyst, catalyst concentration, solvent used, temperature, pressure are the same.

Experimental findings as a function of heating rate and topological constraints are summarized in a schematic drawing shown in Figure 17. The conclusions are as follows:

- Mechanism involved in melting behavior of “disentangled” and entangled polymer changes with the heating rate, Figures 6, 7 and 8. For example in “disentangled” polyethylene, below the heating rate of 1 °C/min melting occurs by successive detachment of chains from side surface, whereas above 1 °C/min melting can occur randomly from the side as well as inside the crystallites.
- The discrete change in slope with the heating rate (below and above 1 °C/min) suggests difference in mechanism involved in crystal melting, where the number of chain segments involved in the melting process also increases with the increasing heating rate (see Figures 6, 7, and 9).
- The kinetics involved in the melting process becomes apparent on annealing the sample at the onset of the melting temperature.
- In the nascent “disentangled” polymer, two different nonlinear logarithmic heating rates showing dependence on peak melting temperature are observed, whereas the nascent entangled sample shows only one nonlinear logarithmic heating rate dependence (see Figure 6, 7 and 9).
- The two different nonlinearity in nascent “disentangled” polymer are associated with (a) melting by successive detachment of chain stems from the crystal surface at low heating rates (<1 °C/min) and (b) cluster melting at higher heating rates (>1 °C/min), where the melting can proceed not only from the surface but also from the crystalline core.
- In nascent entangled polymer at low heating rates (<1 °C/min), melting by successive detachment of the chain stems is not feasible as the same chain is shared among many crystallites and demands co-operative conformational transformation at larger length scales. Thus, the requisite of simultaneous surface and cluster melting requires higher melting temperature compared to the nascent “disentangled” polymer, Figure 6. The concept is shown schematically in Figure 17b.
- The melt-crystallized sample of the nascent polymers melts at lower temperature, satisfying the conventional Gibbs–Thomson equation. The low melting temperature is due to the absence of re-entrant chains that does not require cooperative conformational transformation between the neighboring chains. Hence no heating rate dependence on the melting temperature is observed below 1 °C/min. However, at higher heating rates (>1 °C/min) where melting can occur in clusters the heating rate dependence in melting arises because of cluster melting at different length scales (Figure 7, schematically shown in Figure 17c). These findings at low heating rates are in contradiction with the melting behavior observed in nascent “disentangled” and entangled polyethylene.
- Slope for the heating rate dependence of peak melting temperature increases with a) increasing entanglement density in amorphous region, and b) with the increasing number of shared chains among many crystallites, Figures 6, 7, 8, and 9.
- The annealing of the nascent “disentangled” samples, below peak melting temperature, confirms that synthesized UHMW–PE are close to mono molecular single crystals, which upon annealing (very slow heating rates) melt from the side surfaces by successive detachment of chain stems. These findings are in agreement with the studies performed by Toda et al. on single crystals and are in accordance with our studies at low heating rate, < 1 °C/min.
- However, the melting of chain folded nascent crystals in the vicinity and below their peak melting temperature complicates by the simultaneous process of crystal perfectioning through reorganization. The reorganization process shifts peak melting temperature to higher values and increases the degree of superheating, which is characterized by ΔT_A (=melting temperature – annealing temperature). The increase suppresses melting process via successive detachment of chain stems from the crystal surface and their diffusion in the melt.
- Melting temperature of “disentangled” UHMW–PE polymer increases with increasing molecular weight.
- The characteristic melting time, τ , in nascent “disentangled” samples, decreases with increasing molecular weights due to lower entanglement density in amorphous region of higher M_w samples.

■ ASSOCIATED CONTENT

S Supporting Information. Calculation on the occupancy of UHMW–PE chain in a crystal of specific dimension, endotherms normalised by respective heating rates for disentangled and entangled samples of different M_w of UHMW–PE, and characteristic melting time calculation using TM–DSC. This material is available for free of charge via the Internet at <http://pubs.acs.org>.

■ AUTHOR INFORMATION

Corresponding Author

*Telephone: +44 (0) 1509 223156. Fax: +44 (0) 1509 223949.
E-mail: s.rastogi@lboro.ac.uk.

■ ACKNOWLEDGMENT

This work is part of the Research Program of the Dutch Polymer Institute (DPI), Eindhoven, The Netherlands, Project nr. 637. We are thankful to Dr. Sara Ronca and Mr. Giuseppe Forte for their help with SEM and DSC measurements.

■ REFERENCES

- (1) Till, P., Jr. *J. Polym. Sci.* **1957**, *24*, 301–306.
- (2) Keller, A. *Phil. Mag.* **1957**, *2*, 1171–1175.
- (3) Fischer, E. Z. *Naturforsch.* **1957**, *12a*, 753–754.
- (4) Rånby, B.; Morehead, F.; Walter, N. *J. Polym. Sci.* **1960**, *44*, 349–367.
- (5) Reneker, D.; Geil, P. *J. Appl. Phys.* **1960**, *31*, 1916–1925.
- (6) Bassett, D. C. *J. Cryst. Growth* **1968**, *3–4*, 92–96.
- (7) Wunderlich, B.; Czornyj, G. *Macromolecules* **1977**, *10*, 906–913.
- (8) Rastogi, S.; Lippits, D. R.; Peters, G. W. M.; Graf, R.; Yao, Y.; Spiess, H. W. *Nat. Mater.* **2005**, *4*, 635–641.
- (9) Muthukumar, M. In *Interphases and Mesophases in Polymer Crystallization III*; Springer: Berlin and Heidelberg Germany, 2005; Vol. 191, p 241.
- (10) Muthukumar, M. In *Progress in Understanding of Polymer Crystallization; Lecture Notes in Physics*, Springer: Berlin and Heidelberg Germany, 2007, Vol. 714, p 1.
- (11) Höhne, G. *Polymer* **2002**, *43*, 4689–4698.
- (12) Strobl, G. *Eur. Phys. J. E* **2000**, *3*, 165–183.
- (13) Strobl, G. *Prog. Polym. Sci.* **2006**, *31*, 398–442.
- (14) Keller, A.; Hikosaka, M.; Rastogi, S.; Toda, A.; Barham, P.; Goldbeck-Wood, G. *J. Mater. Sci.* **1994**, *29*, 2579–2604.
- (15) Toda, A.; Kojima, I.; Hikosaka, M. *Macromolecules* **2008**, *41*, 120–127.

- (16) Hellmuth, E.; Wunderlich, B. *J. Appl. Phys.* **1965**, *36*, 3039–3044.
- (17) Toda, A.; Hikosaka, M.; Yamada, K. *Polymer* **2002**, *43*, 1667–1679.
- (18) Danley, R. L.; Caulfield, P. A. *Proc. 29th Conf. N. Am. Therm. Anal. Soc.* **2001**, *268*, 673–678.
- (19) Lippits, D.; Rastogi, S.; Höhne, G. *Phys. Rev. Lett.* **2006**, *96*, 1–4.
- (20) Rastogi, S.; Lippits, D. R.; Höhne, G. W. H.; Mezari, B.; Magusin, P. C. M. *J. Phys: Condens Mat* **2007**, *19*, 205122.
- (21) Lippits, D. R. Controlling the melting kinetics of polymers; A route to a new melt state, Eindhoven University of Technology: Eindhoven, The Netherlands, 2007.
- (22) Toda, A.; Tomita, C.; Hirosaka, M. *J. Therm. Anal. Calorim.* **1998**, *54*, 623–635.
- (23) Toda, A.; Tomita, C.; Hikosaka, M.; Saruyama, Y. *Polymer* **1998**, *39*, 5093–5104.
- (24) Talebi, S. Disentangled Polyethylene with Sharp Molar Mass Distribution; Implications for Sintering, Technische Universiteit Eindhoven: Eindhoven, The Netherlands, 2008.
- (25) Gill, P.; Sauerbrunn, S.; Reading, M. *J. Therm. Anal. Calorim.* **1993**, *40*, 931–939.
- (26) Reading, M.; Elliott, D.; Hill, V. *J. Therm. Anal. Calorim.* **1993**, *40*, 949–955.
- (27) Reading, M.; Luget, A.; Wilson, R. *Thermochim. Acta* **1994**, *238*, 295–307.
- (28) Wunderlich, B.; Jin, Y.; Boller, A. *Thermochim. acta* **1994**, *238*, 277–293.
- (29) Boller, A.; Jin, Y.; Wunderlich, B. *J. Therm. Anal.* **1994**, *42*, 307–330.
- (30) Di Lorenzo, M.; Wunderlich, B. *Thermochim. acta* **2003**, *405*, 255–268.
- (31) Toda, A.; Tomita, C.; Hikosaka, M.; Saruyama, Y. *Thermochim. Acta* **1998**, *324*, 95–107.
- (32) Toda, A.; Arita, T.; Tomita, C.; Hikosaka, M. *Thermochim. Acta* **1999**, *330*, 75–83.
- (33) Toda, A.; Arita, T.; Hikosaka, M. *J. Mater. Sci.* **2000**, *35*, 5085–5090.
- (34) Toda, A.; Arita, T.; Hikosaka, M. *Thermochim. Acta* **2005**, *431*, 98–105.
- (35) Minakov, A. A.; Mordvintsev, D. A.; Tol, R.; Schick, C. *Thermochim. Acta* **2006**, *442*, 25–30.
- (36) Pak, J.; Pyda, M.; Wunderlich, B. *Macromolecules* **2003**, *36*, 495–499.
- (37) Righetti, M. C.; Lorenzo, M. L. D.; Tombari, E.; Angiuli, M. *J. Phys. Chem. B* **2008**, *112*, 4233–4241.
- (38) Di Lorenzo, M. L.; Righetti, M. C.; Cocca, M.; Wunderlich, B. *Macromolecules* **2010**, *43*, 7689–7694.
- (39) Schick, C.; Wurm, A.; Mohamed, A. *Colloid Polym. Sci.* **2001**, *279*, 800–806.
- (40) Lu, S. X.; Cebe, P. *Polymer* **1996**, *37*, 4857–4863.
- (41) Di Lorenzo, M. L. *Polymer* **2009**, *50*, 578–584.
- (42) Pandey, A.; Champouret, Y.; Rastogi, S. *Macromolecules* **2011**, *44*, 4952–4960.
- (43) Talebi, S.; Duchateau, R.; Rastogi, S.; Kaschta, J.; Peters, G. W. M.; Lemstra, P. J. *Macromolecules* **2010**, *43*, 2780–2788.
- (44) Tervoort-Engelen, Y.; Lemstra, P. J. *Polym. Commun.* **1991**, *32*, 343–345.
- (45) Schawe, J. *Thermochim. Acta* **1993**, *229*, 69–84.
- (46) Yao, Y.-F.; Graf, R.; Spiess, H. W.; Rastogi, S. *Macromolecules* **2008**, *41*, 2514–2519.
- (47) Yao, Y.-F.; Graf, R.; Spiess, H.; Lippits, D.; Rastogi, S. *Phys. Rev. E* **2007**, *76*, 1–4.
- (48) Yao, Y.; Graf, R.; Spiess, H.; Rastogi, S. *Macromol. Rapid Commun.* **2009**, *30*, 1123–1127.
- (49) Rastogi, S.; Yao, Y.; Ronca, S.; Bos, J.; van der Eem, J. *Macromolecules* **2011**, *44*, 5558–5568.
- (50) Lippits, D. R.; Rastogi, S.; Höhne, G. W. H.; Mezari, B.; Magusin, P. C. M. *Macromolecules* **2007**, *40*, 1004–1010.